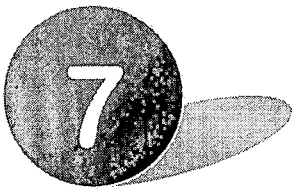

Dasatinib and MCM-41 MSNs

Materials and Methods

7.1 Synthesis of Mesoporous MCM-41 MSNs

Mesoporous MCM-41 MSNs were synthesized as described in section 5.1.

7.2 Characterization of Mesoporous MCM-41 MSNs

Mesoporous MCM-41 MSNs were characterized as described in section 5.2.

7.3 Drug-Dasatinib loading in MCM-41 MSNs

Synthesized MCM-41 MSNs were used for dug loading process. MSNs were dried in oven at 100 °C for 30 min in order to remove moisture from the pores. The drug loading was carried out by direct impregnation method. The MSNs was placed as powder into the drug solution of the drug with a given concentration. The drug loading procedure is described below.

In preliminary drug loading procedure, dasatinib (DTB) (300 mg) was dissolved in an appropriate solvent (10 ml) and then MCM-41 MSNs (200 mg) was added. The mixture was kept under magnetic stirring at room temperature for 24h and then was left to settle for 2h to allow the sedimentation of the fine precipitate that was collected by filtration. The recovered solid was dried for 24h under vacuum at room temperature and stored at room temperature.

The drug loaded MSNs were analyzed by XRD, nitrogen adsorption isotherm, surface area, FT-IR spectroscopy and DSC analysis. The loading efficiency (LE) within the MCM-41 MSNs was determined indirectly by determining the amount of non- entrapped or non- adsorbed drug, by measuring concentration of DTB in the solvent and in the washing solutions. The drug loading efficiency was analyzed spectrophotometrically (Shimadzu-1700, Japan) at 329 nm. Suitable dilution factor was applied and the loading efficiency was calculated according to the formula[1] given below.

$$Wt\% = \frac{m1 - \frac{50}{v}CV}{m2 + \left(m1 - \frac{50}{v}CV\right)} \times 100$$

Where, m1 and m2 correspond to the initial mass of DTB and mesoporous materials added into 0.1 M HCl solution. C is the concentration of filtrates diluted in 50 ml volumetric flask, v is sampled volume from filtrates, and V is the volume of 0.1 M HCl solution for drug loading.

7.3.1 Optimization of drug loading procedure

The process of drug loading was optimized with respect to solvent, drug: carrier ratio, temperature, time, and stirring rate.

□***Solvent***

Solvent optimization involves the use of different solvents for drug loading and was checked for % of drug load. The main selection criterion was that the solvent should give optimum solubility of drug and minimum or no solubilization of carrier.

□***Ratio of drug and drug carrier***

Another important parameter is to select proper ratio of drug (DTB) and drug carrier (MCM-41) for maximum entrapment. Different ratio were tried and checked for drug loading.

□***Temperature and time***

Temperature and soaking/stirring time are two important parameters which may affect drug loading. Drug (DTB) loading procedure was carried out at two different temperature i.e. room temperature and 40° C. Similarly, five different time durations were selected i.e. 6h, 12h, 24h, 48h, and 72h for drug loading process.

□***Stirring rate***

Rate of stirring also greatly affect the drug loading, hence it is important to optimize the stirring rate. Effect of stirring at higher and normal rate is studied by using magnetic stirrer.

7.3.2 Factorial design for drug loading optimization

3^3 factorial design was used to determine the effect of the three independent factors: the concentration of drug solution, the stirring rate, and drug: carrier weight ratio on the % drug loading of MCM-41 MSNs. Each factor was tested at three levels of low, medium and high, designed as -1, 0, and +1 respectively.

Microsoft Excel was used for multiple regression calculation in order to deduce the factors having significant effect on the formulation properties. Three-dimensional response surface plots and two dimensional contour plots resulting from equations were obtained by the NCSS software.

7.3.3 Evaluation of drug loaded MCM-41 MSNs

Drug loaded MSNs were evaluated by similar instrumental techniques as described in section 5.2.

7.4 *In-Vitro* dissolution study

In-vitro drug release from the MSNs was studied by the rotating paddle method at 50 rpm (Veego dissolution test apparatus- basket type USP), 37±0.5 °C and in sink conditions. Tests were performed in the following dissolution media[3]: simulated gastric fluid at pH 1.2±0.1, phosphate buffer at pH 4.5±0.1, phosphate buffer at pH 6.8±0.1, simulated intestinal fluid at pH 7.4±0.1 and acetate buffer pH 4 + Triton X-100 (1%) as reported dissolution media[2]. Drug release was monitored for 1 h and compared to DTB crystalline powder, the physical mixture and market formulation. Five milliliters of dissolution fluid was removed from the vessel at predetermined intervals and replaced by the same volume of fresh dissolution medium. The samples were filtered through PTFE 0.45 μm filters and DTB content was determined by UV spectrophotometry (λ max = 329 nm for pH 1.2, λ max = 325 nm for pH 4.5, λ max = 325 nm for pH 6.8, λ max = 325 nm for pH 7.4, λ max = 322 nm for reported dissolution media). All experiments were performed in triplicate and the error was expressed as standard deviation.

Results and Discussion

It was found that the synthesized MCM-41 MSNs are structurally smooth and characterizations data showed well developed mesostructure and mesoporosity. The developed MCM-41 MSNs were used for the drug (dasatinib) loading.

7.5 Drug-Dasatinib loading in MCM-41 MSNs

Due to the high specific areas and pore volumes of MSNs, large quantities of drug can be incorporated into the porous MSNs by adsorption to the pore or/and surface of MSNs. The MCM-41 MSNs were added to a concentrated solution of the DTB and the suspension was stirred for about 24h for maximum diffusion of the drug molecules into the mesopores (Fig. 7.1).

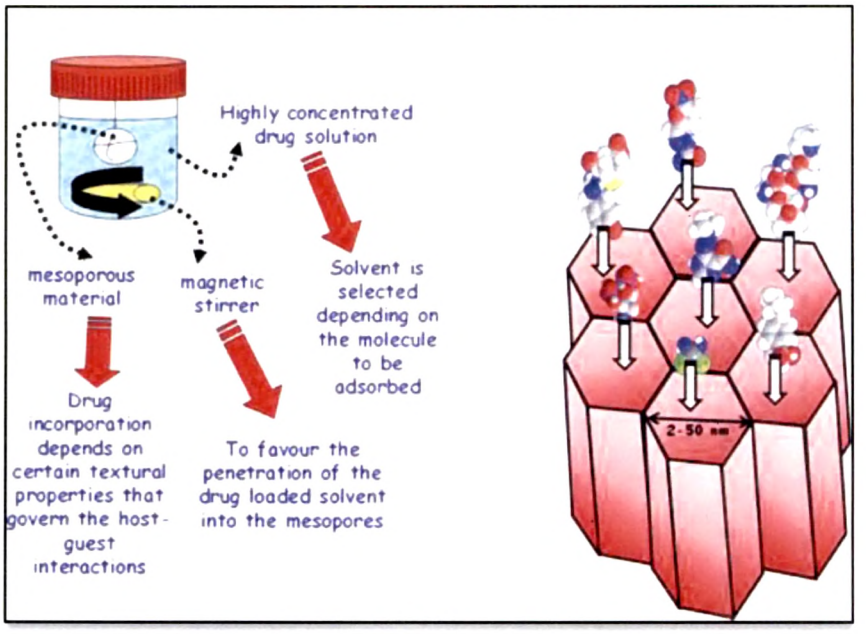

Figure 7.1: Schematic representation of the drug loading procedure

Several factors need to be optimized to achieve maximum drug loading. The right pore size of the synthesized MCM-41 MSNs is important as it determines the size of the molecules which can be adsorbed into the mesopores.

It is important to know whether drug molecules are adsorbed in the pores or on the surface of MSNs as it can later on affect the release characteristics. Normally, pore/drug size ratio>1 allows the adsorption of drug inside the pores[3]. It is reported that the molecular size of DTB is ~ 3.1 nm[4] and the data of nitrogen adsorption isotherm indicated the pore size of MCM-41 MSNs as 3.6 nm giving the pore/drug size ratio as 1.16, indicating that, DTB molecules can be adsorbed in the pores of synthesized MCM-41 MSNs.

The drug loading into the MCM-41 MSNs is also controlled by the chemical nature of the pores and pore walls. The inorganic networks of MCM-41 MSNs have plenty of silanol groups (Si-OH), present into the mesopores and on the surface (Fig. 7.2) that would interact (through hydrogen bond) with the functional groups of the drug[4, 5]. Attracting interaction between the silanol group of MSNs and functional group of the drug, the drug molecules either confined within the pores or they adsorbed to the surface of MSNs[3].

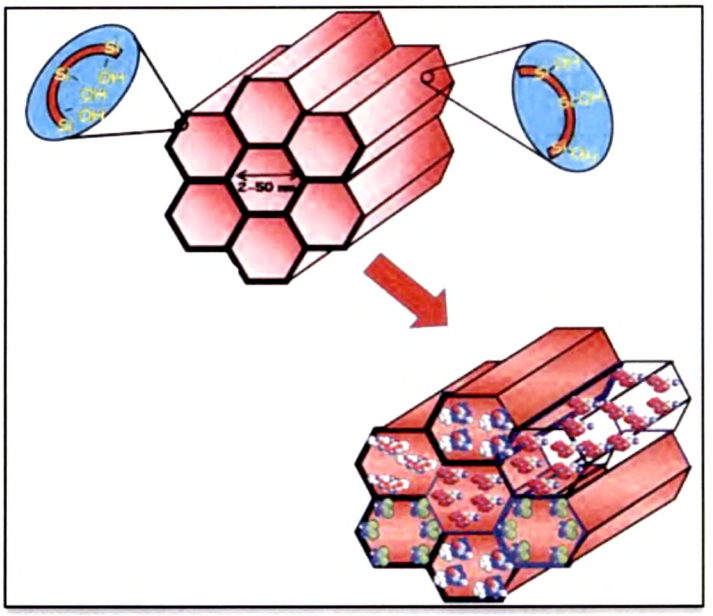

Figure 7.2: Textural properties and drug loading and/or adsorption on MSNs

The probable mechanism of drug loading is that, the a nitrogen present on piperazine ring of DTB structure would form hydrogen bonds with the silanol groups of MCM-41 MSNs and consequently drug molecules would be retained into themesopores[7, 9](Fig. 7.3).

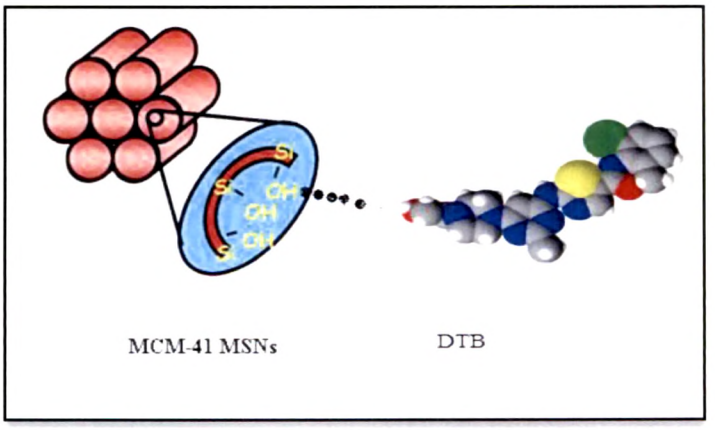

Figure 7.3: DTB linkage to silanol group of MCM-41 MSNs

The drug loading process was also optimized for solvent, ratio of drug and drug carrier (MSNs), temperature, time and stirring rate.

7.5.1 Optimization of drug loading procedure

□***Solvent***

Right selection of solvent is necessary for maximum drug loading as discussed in 5.6.1. Three solvents were tried for DTB loading. As DTB is prominently soluble in acidic media[2], solutions of mineral acids and acidic buffer solutions were tried. Different solvents tried were acetate buffer pH 2.8, 0.1 M HCl and 0.5 M HCl. Drug loading was carried out with these selected solvents and % LE was checked. The results are shown in Table 7.1 and Fig. 7.4

Table 7.1: Effects of different solvents on MCM-41 MSNs drug loading

Solvent used for drug loading	% Drug loading in MCM-41 MSNs
Acetate buffer pH 2.8	29. 587
0.1 M HCl	48. 124
0.5 M HCl	47. 754

Results suggest that the drug loading is maximum when 0.1 M HCl was used as a solvent.

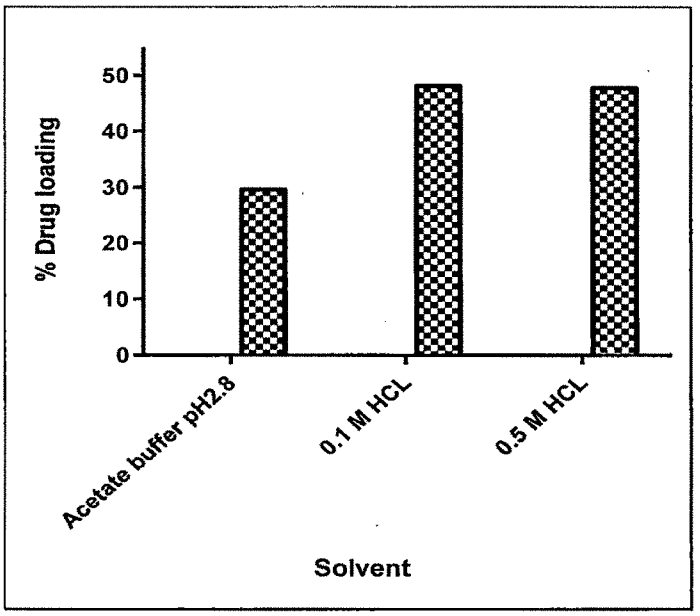

Figure 7.4: Effects of different solvents on MCM-41 MSNs drug loading

□*Ratio of drug and drug carrier*

Weight ratio of drug to MSNs can greatly affect drug loading ability. It was necessary to find out the optimum drug to MSNs ratio. To optimize the ratio, different proportion of MSNs to drug was taken as mentioned in Table 7.2.

Table 7.2: Effects of drug: MSNs ratio on MCM-41 MSNs drug loading

Weight ratio Drug : Carrier	% Drug loading in MCM-41 MSNs
1: 0.5	25. 687
1:1	47. 862
1: 1.5	38. 090
1: 2	30. 915

Ratio was optimized by taking fixed proportion of drug and variable proportion of MSNs. Four different drug: MSNs proportions were tested i.e. 0.5, 1, 1.5, and 2. It was found that maximum drug entrapment was achieved with 1:1 weight ratio. The optimization data graphically present in Fig. 7.5.

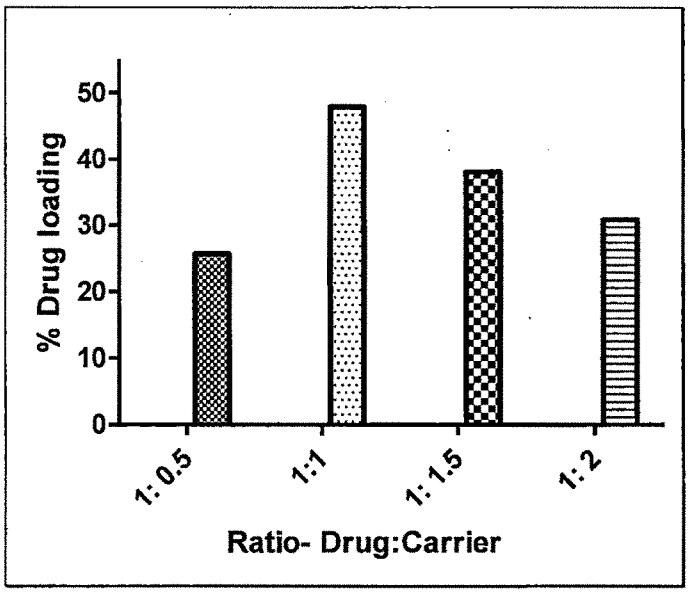

Figure 7.5: Effects of drug: MSNs ratio on MCM-41 MSNs drug loading

□*Temperature and time*

Suitable temperature and stirring time required for maximum drug loading was determined. The loading process was carried out at two different temperature i.e. room temperature and 40 °C. Similarly five different time durations were selected for proper agitation during the loading process. Stirring was provided with magnetic stirrer for five different time duration, i.e. 6h, 12h, 24h, 48h, and 72h. The results are summarized in Table 7.3 and Fig. 7.6.

Table 7.3: Effects of temperature and time on MCM-41 MSNs drug loading

Temperature	% of Drug loading at different time duration				
	6h	12h	24h	48h	72h
Room temp.	46. 356	47. 253	47. 852	47. 652	47. 102
40° C	41. 681	42. 268	47. 450	45. 371	44. 102

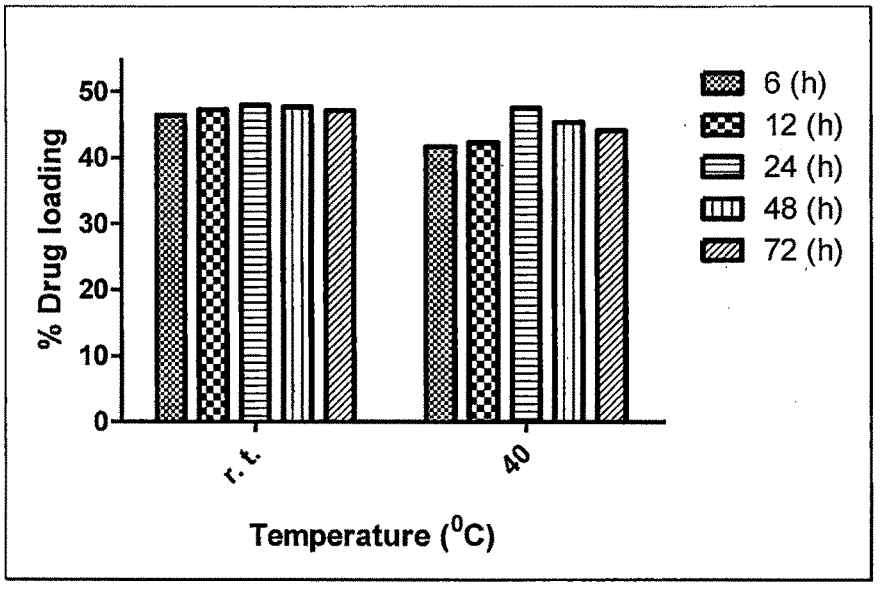

Figure 7.6: Effects of temperature and time on MCM-41 MSNs drug loading

The results of % LE revealed that maximum drug loading was attainable if the MSNs and DTB were continuously agitated for 24h.

The results of drug loading at 40° C suggested that the elevated temperature did not show any significant effect on drug loading. Higher temperature may increase the DTB solubilization but at elevated temperature the drug molecules may experience high Brownian motion[7-9] which may not allow the easy diffusion and adsorption in the mesopores of MCM-41 MSNs.

□*Stirring rate*

During the loading process, the solution is continuously stirred using magnetic stirrer to improve access of the concentrated solution to the mesopores[5]. MSNs sample was added in drug solution with vigorous stirring and vigorous stirring was continued for 1h, followed by gentle stirring for 23h.

Vigorous stirring was provided at 800 rpm, whereas the gentle stirring rate was optimized at four levels i.e. 50 rpm, 100 rpm, 200 rpm and 400 rpm. The results are summarized in Table 7.4 and graphically presented in Fig. 7.7. The results revealed that as stirring rate was increased from 100 rpm to 400 rpm; the rate of drug loading was decreased from 47 to 34 %. Optimized stirring rate data suggested that for the maximum drug loading the stirring should be 100 rpm.

Table 7.4: Effects of stirring rate on MCM-41 MSNs drug loading

Stirring speed	~50 rpm	~100 rpm	~200 rpm	~400 rpm
% Drug loading	45.554	47. 902	41. 825	34. 632

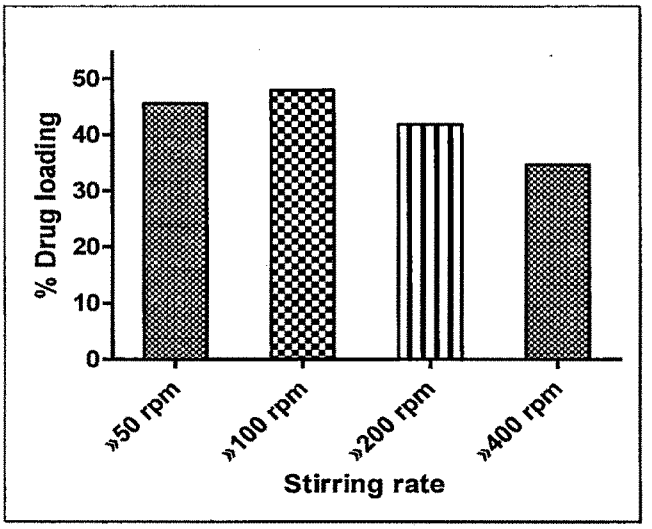

Figure 7.7: Effects of stirring rate on MCM-41 MSNs drug loading

7.5.2 Factorial design for drug loading optimization

The process of drug loading was optimized with respect to different influencing variables such as solvent, ratio of drug: carrier, temperature, time, and stirring rate. The conventional method of optimization involves the study of effect of different factors on formulation by changing one variable at a time (OVAT). Since the combined effects of variables are not evaluated, so it is difficult to formulate an ideal pharmaceutical formulation. The complexity of process variables was studied

using a factorial design[10] and a statistical model was developed to study the effect of stirring rate, weight ratio of drug: carrier and concentration of drug solution on formulation characteristics.

7.5.2.1 Preparation of batches and optimization by factorial design

Twenty-seven batches of DTB loaded MCM- 41 MSNs (as a carrier) were prepared using 3^3 factorial design by varying three independent variables; the concentration of drug solution (X1), the stirring rate (X2), and drug: carrier ratio (X3). Each factor was tested at three levels of low, medium and high, designed as -1, 0, and +1 respectively. The normalized factor levels of independent variables are given in Table 7.5.

Table 7.5: Factorial 3^3: factors, their levels, and transformed values

Variables with transformed value	Levels		
	Low (-1)	Medium (0)	High (1)
(X1) Concentration of drug solution (mg/ml)	1	10	20
(X2) Stirring rate (rpm)	10	50	100
(X3) Ratio drug: carrier	0.25	0.5	1

The % DTB loading efficiency (response variable) of the prepared batches was determined (Table 7.6) and the highest percent drug loading achieved in MCM- 41 MSNs was 48% at 1 level of X1 (20 mg/ml), 1 level of X2 (100 rpm), and 1 level of X3 (1:1 weight ratio). The results were subjected to multiple-regression analysis. The fitted equation related to percent loading efficiency and transformed factors is given in Eq. (1).

$$Y = 14.519 + 12.588X1 + 7.595X2 + 4.165X3 + 2.682X1^2 + 1.264X2^2 + 1.238X3^2 + 3.449X1X2 + 2.470X1X3 - 0.258X2X3 - 1.264X1X2X3 \quad (1)$$

Table 7.6: Different batches with their experimental coded level of variables for 3^3 factorial design

Batch code	X1= Concentration of drug solution	X2= Stirring rate	X3= Ratio drug: carrier	% drug loading
M1	-1	-1	-1	1.867
M2	-1	-1	0	2.109
M3	-1	-1	1	2.638
M4	-1	0	-1	2.761
M5	-1	0	0	5.968
M6	-1	0	1	7.597
M7	-1	1	-1	9.155
M8	-1	1	0	11.987
M9	-1	1	1	12.458
M10	0	-1	-1	8.875
M11	0	-1	0	9.125
M12	0	-1	1	10.741
M13	0	0	-1	11.896
M14	0	0	0	15.652
M15	0	0	1	19.321
M16	0	1	-1	21.951
M17	0	1	0	22.367
M18	0	1	1	25.764
M19	1	-1	-1	12.926
M20	1	-1	0	19.588
M21	1	-1	1	29.358
M22	1	0	-1	21.887
M23	1	0	0	24.493
M24	1	0	1	44.628
M25	1	1	-1	39.167
M26	1	1	0	43.069
M27	1	1	1	48.019

The data indicated that percent loading efficiency is more dependent on the concentration of drug solution and the stirring rate than the ratio of drug: carrier. The value of correlation coefficient (r) was found to be 0.978, indicating a good fit. The small values of coefficients of terms $X2^2$, $X3^2$, X2X3, and X1X2X3 (Eq. 2), were least contributing in loading of DTB in MCM-41 MSNs ($p>0.05$). Hence, they were

omitted to evolve the reduced model (Eq. 2). The summary of regression analysis is shown in Table 7.7.

$$Y= 16.188 + 12.588X1 + 7.595X2 + 4.165X3 + 2.682X1X2 + 2.470X1X3 \quad (2)$$

The positive sign for the coefficient of X1, X2, and X3 in Eq. (2) showed that the percent drug loading can be increased by an increase in X1, X2, and X3. The results of ANOVA of the second-order polynomial equation are given in tables 7.7.

Table 7.7: Analysis of variance (ANOVA) of variables for full and reduced model of MCM-41 MSNs

	DF	SS	MS	F	R	R^2	Adj.R^2
Regression							
FM	10	4441.404	444.140	36.797	0.978	0.958	0.932
RM	5	4266.217	853.243	48.649	0.959	0.920	0.901
Error							
FM	16	193.120	12.070				
RM	21	368.307	17.538				

[SSE2–SSE1 = 368.307–193.120= 175.187
No. of parameters omitted = 05
MS of error (full model) = 12.070
F calculated = (SSE2–SSE1/no. of parameters omitted)/MS of error (full model)
= (175.187/5)/12.070 = 2.801
Tabled F value = 2.85 (α = 0.05, V1 = 5, and V2 = 16).
a Where DF indicates degrees of freedom; SS sum of square; MS mean sum of square and F is Fischer's ratio].

F-Statistic of the results of ANOVA of full and reduced model confirmed omission of non-significant terms of Eq. (1) and (2). Since the calculated F value (2.801) was less than the tabled F value (2.85), it was concluded that the neglected terms do not significantly contribute in the prediction. The goodness of fit of the model was checked by the determination coefficient (R^2). In this case, the values of the determination coefficients (R^2) and adjusted determination coefficients (adj R^2) were very high (>90%), which indicates a significance of the model. All the above considerations indicate an adequacy of the regression model[11, 12].

7.5.2.2 Contour plots

Figure 7.8 (a–i) are the contour plot for DTB loaded MCM- 41 MSNs which were found to be linear and signifying linear relationship between variables X1, X2, and X3. It was observed from contour plots (Fig. 7.8-c) that maximum LE (48.019%) could be obtained with X2 between 0.5 level (50 rpm) to 1 level (100 rpm) and X3 between 0.5 level (0.5:1) to 1 level (1:1). Fig. 7.8-f revealed that maximum loading could be obtained with X1 between 0.6 level (6 mg) to 1 level (20 mg) and X3 between 0.5 level (0.5:1) to 1 level (1:1). Fig. 7.8-i showed that maximum loading could be obtained with X1 between 0.6 level (6 mg) to 1 level (20 mg) and X2 between 0.5 level (50 rpm) to 1 level (100 rpm). All the two-dimensional contour plots were found to follow the linear relationship between X1, X2, and X3 variables. From the contour, it was observed that higher drug concentration (20 mg/ml), maximum stirring rate (100 rpm), and unit weight ratio of drug: carrier are necessary for maximum drug loading.

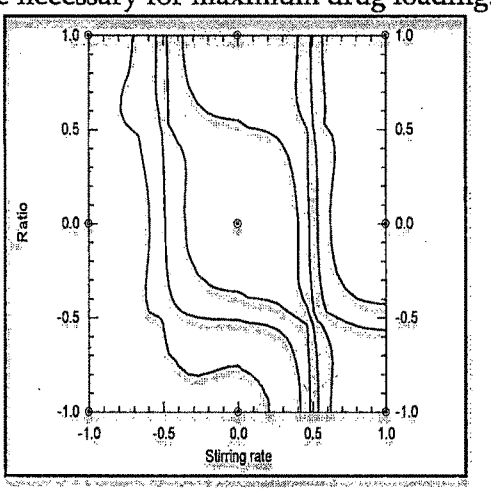

(a) Effect on LE at -1 level of X1

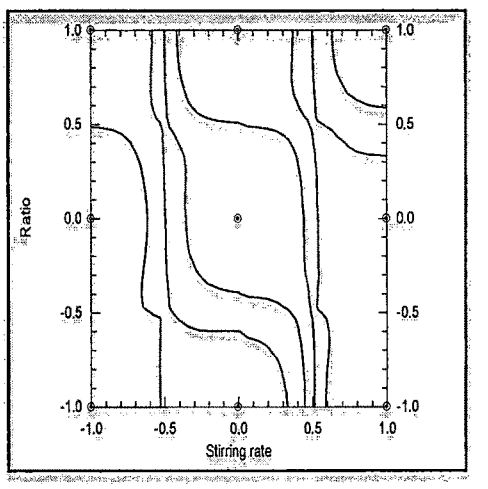

(b) Effect on LE at 0 level of X1

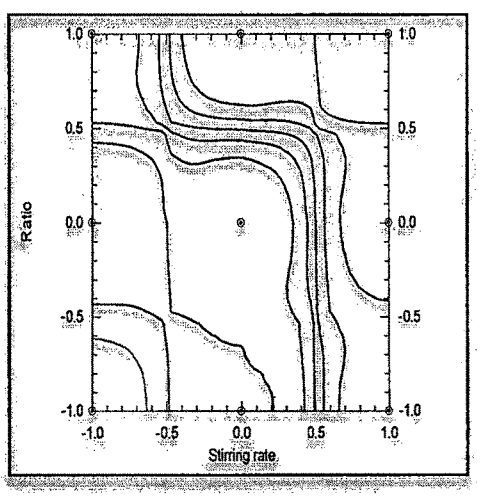

(c) Effect on LE at +1 level of X1

Figure 7.8 (a-c): Contour plots: Effect on LE at -1, 0 and +1 levels of drug concentration (X1)

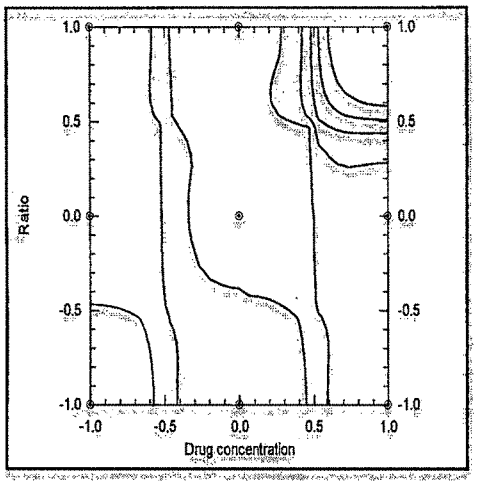

(d) Effect on LE at -1 level of X2

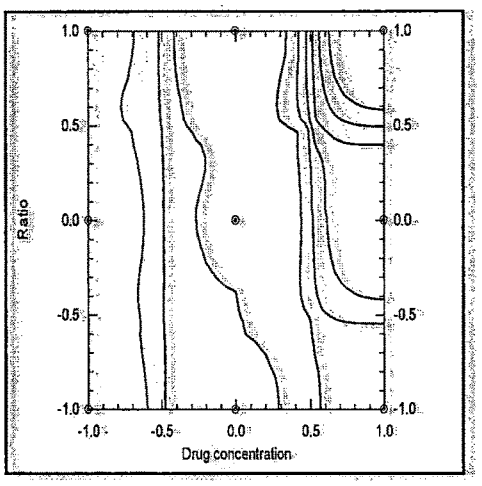

(e) Effect on LE at 0 level of X2

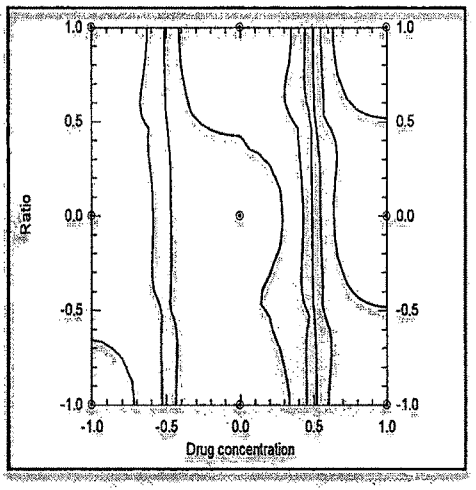

(f) Effect on LE at +1 level of X2

Figure 7.8 (d-f): Contour plots: Effect on LE at -1, 0 and +1 levels of stirring rate (X2)

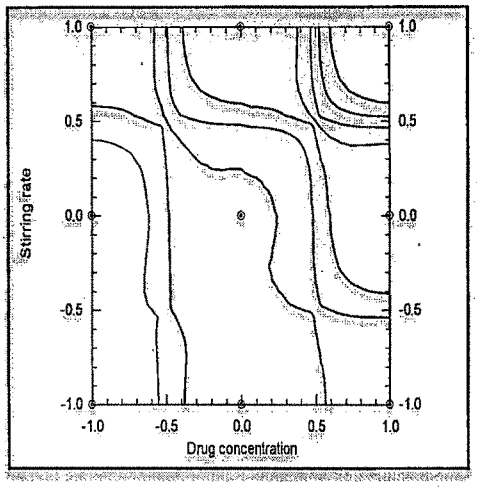

(g) Effect on LE at -1 level of X3

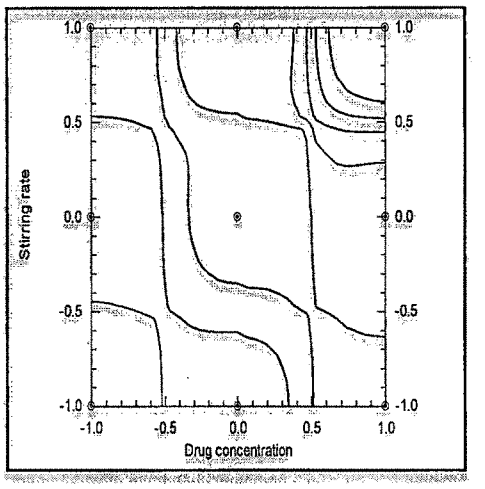

(h) Effect on LE at 0 level of X3

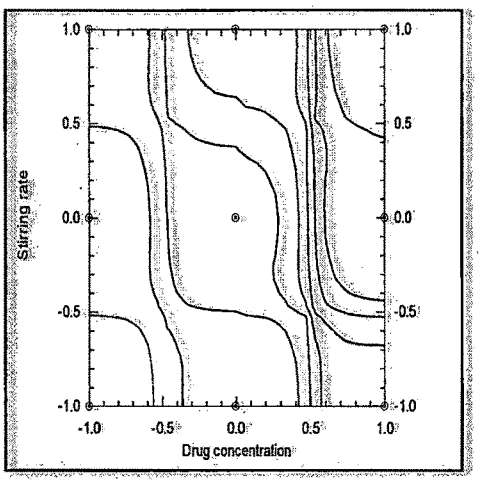

(i) Effect on LE at +1 level of X3

Figure 7.8 (g-i): Contour plots: Effect on LE at -1, 0 and +1 level of drug: carrier ratio (X3)

7.5.2.3 Response surface plots

Three-dimensional response surface plots generated by the NCSS software are presented in Fig. 7.9 (a-i), for DTB loaded MCM- 41 MSNs. Fig. 7.9 (a- c) depict response surface plots for LE of MCM- 41 MSNs at constant level of the factor X1 showing an increase in LE with increase in the stirring rate and increase in weight ratio of drug: carrier. Fig. 7.9 (d- f) depict response surface plots for LE at constant level of the factor X2 indicating an increase in LE with increase in the drug concentration and increase in weight ratio of drug: carrier. Fig. 7.9 (g- i) depict

response surface plots for LE at constant level of the factor X3 suggesting an increase in drug concentration and increase in stirring rate increases the LE.

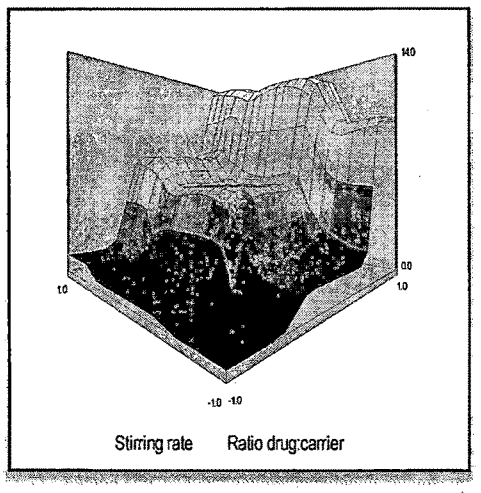

(a) Effect on LE at -1 level of X1

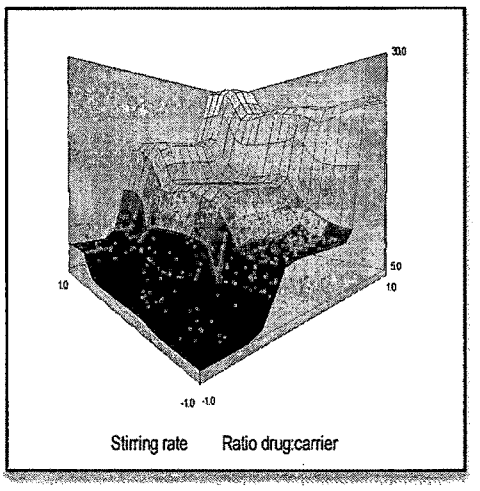

(b) Effect on LE at 0 level of X1

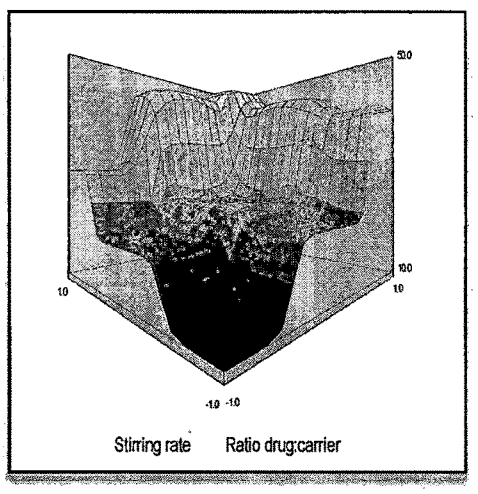

(c) Effect on LE at +1 level of X1

Figure 7.9 (a-c): Response surface plots: Effect on LE at -1, 0 and +1 level of drug concentration (X1)

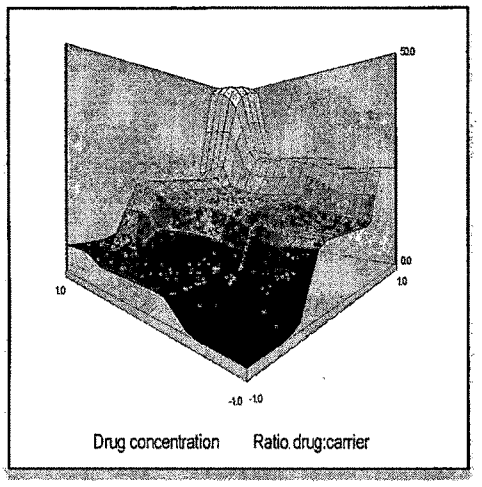

(d) Effect on LE at -1 level of X2

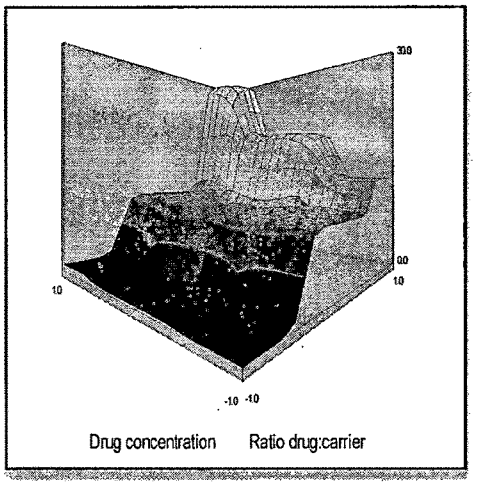

(e) Effect on LE at 0 level of X2

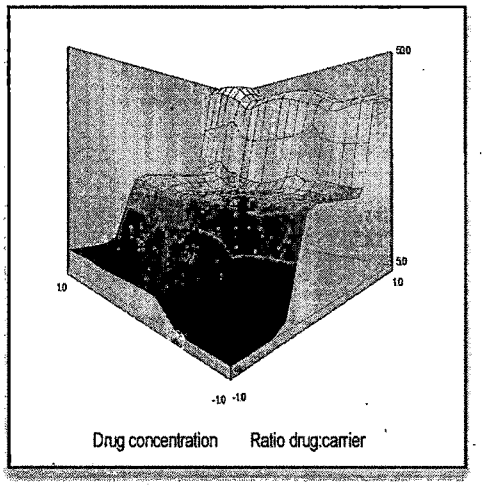

(d) Effect on LE at +1 level of X2

Figure 7.9 (d-f): Response surface plots: Effect on LE at -1, 0 and +1 level of stirring rate (X2)

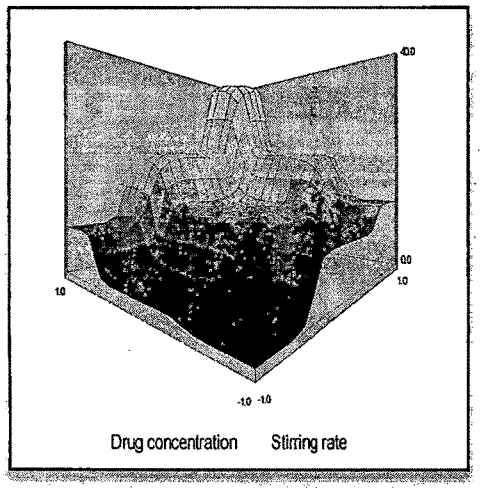

(g) Effect on LE at -1 level of X3

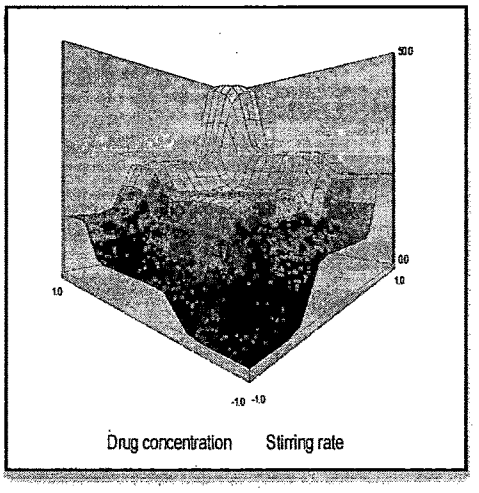

(h) Effect on LE at 0 level of X3

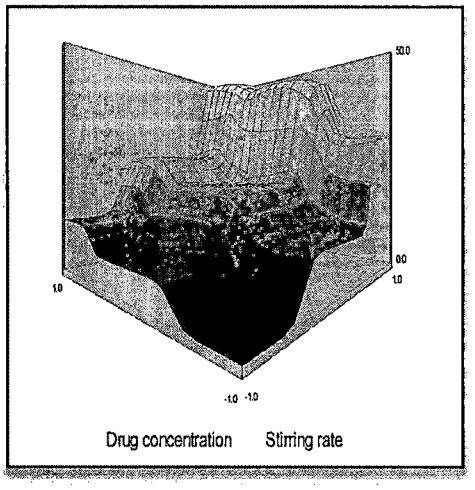

(i) Effect on LE at +1 level of X3

Figure 7.9 (g-i): Response surface plots: Effect on LE at -1, 0 and +1 level of drug: carrier ratio(X3)

7.5.3 Evaluation of drug loaded MCM-41 MSNs

Mesoporous MCM-41 MSNs were evaluated for maximum drug loading and intact mesoporosity. Different instrumental techniques like TEM, XRD, nitrogen adsorption, FTIR and DSC were used for this purpose.

7.5.3.1 Transmission electron microscopy (TEM)

The first step was to check that the mesostructure of the MCM-41 MSNs has survived after the loading process. The MSNs sample was analyzed by TEM. The high resolution TEM images confirmed the prevalence of the ordered

mesostructure after the loading step (Fig. 7.10). TEM Images are marked with some dark spots, which may be the indicative of the confinement of drug molecules within the pores.

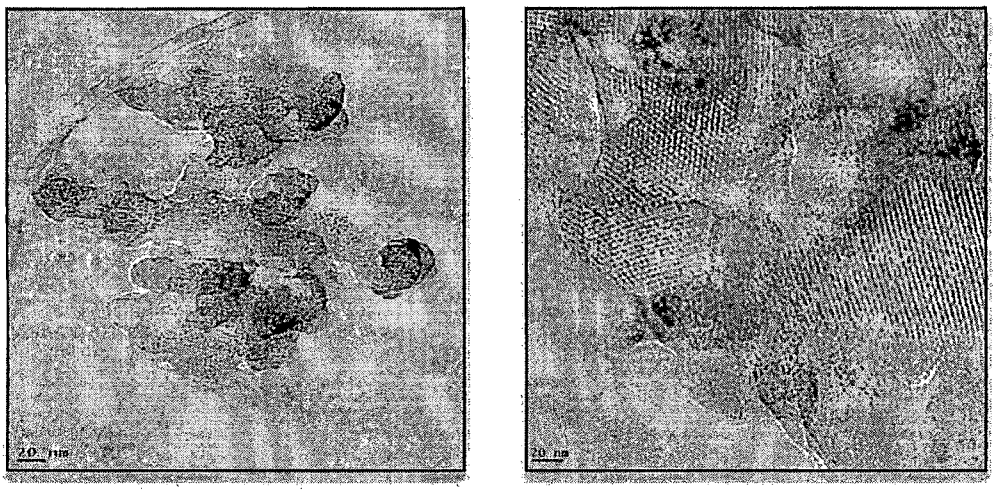

Figure 7.10: TEM images of MSNs after drug loading

7.5.3.2 Powder X-ray diffraction (XRD)

The survival of mesoporosity of the MSNs was further confirmed by XRD. For this purpose, a small angle XRD pattern was carried out before and after the loading process (Fig. 7.11 and 7.12). The mesoporous structure of the MSNs was confirmed by the diffraction peaks at 100, 110 and 200. The same characteristic diffraction peaks were observed in MSNs even after the drug loading process. The presence of peaks was indicated that the mesostructure of MSNs was not disturbed after the drug loading. The XRD pattern of DTB is also shown in Fig. 7.12. The drug loaded MSNs show lack of DTB characteristic peaks in XRD pattern further confirming the entrapment of drug molecules within the mesopores.

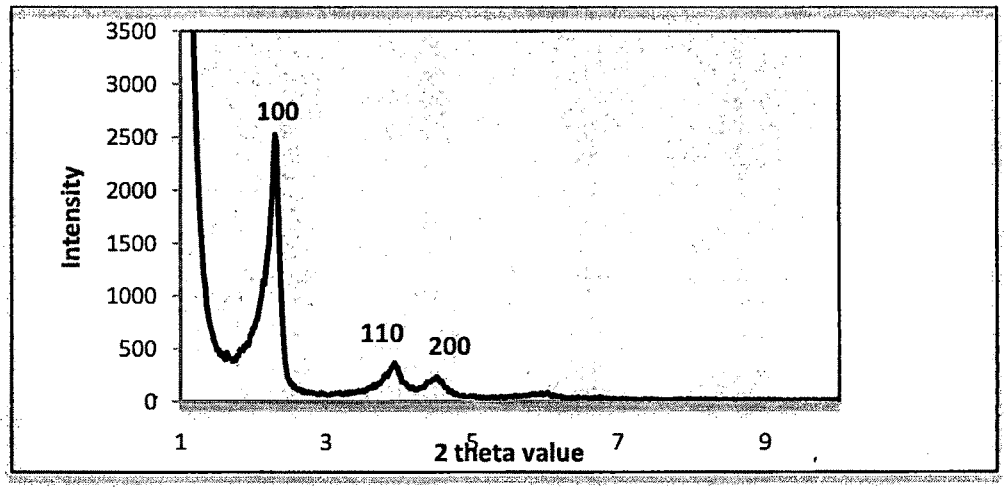

Figure 7.11: XRD pattern of MCM-41 MSNs before the drug loading

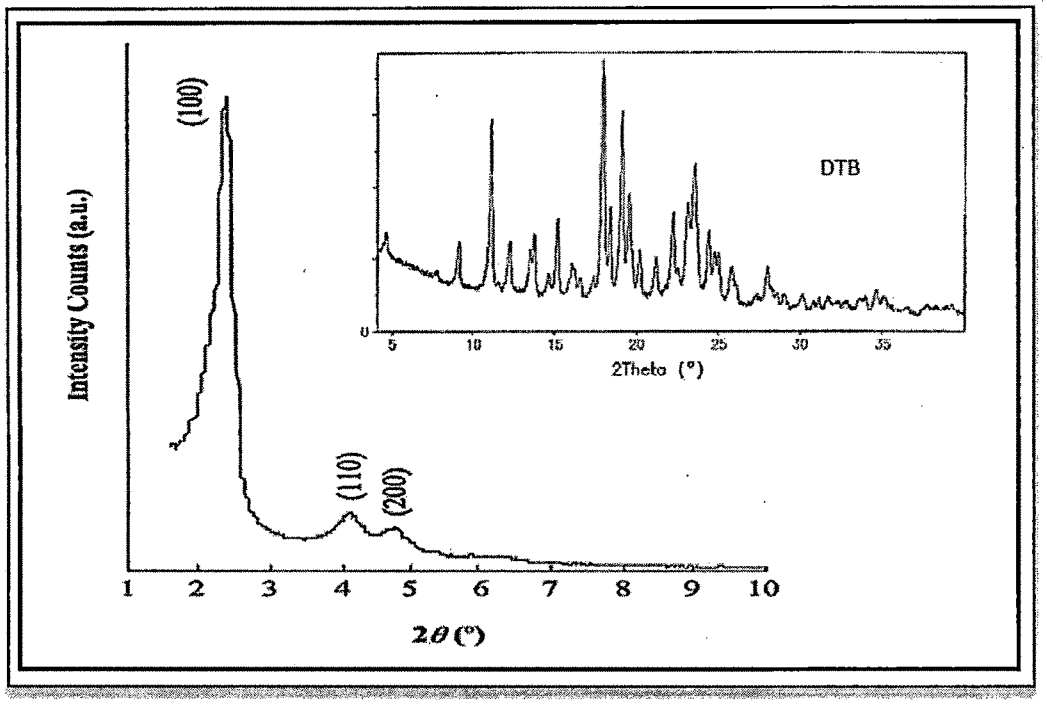

Figure 7.12: XRD pattern of DTB and MCM-41 MSNs after the drug loading

7.5.3.3 Nitrogen adsorption isotherm (BET surface analysis)

After the confirmation of the integrity of the mesostructure, next important point was to check whether the drug molecules are confined inside the mesopores or they are just on the outer surface of the MSNs. Nitrogen adsorption analysis was performed to find out the status of drug molecules. The nitrogen adsorption isotherms were obtained for the pore size distribution and the pore volume determination of MSNs, before and after the loading process.

The pore volume and surface area are normally decreased as a consequence of the MSNs–drug interaction. It can be noted from Fig. 7.14 that the available pore volume was decreased after the drug loading. Decrease in pore volume suggested that the drug molecules are partially filling the mesopores, i.e. the drug molecules are being confined inside the pores[13].

In Fig. 7.13-a and 7.13-b nitrogen adsorption-desorption isotherms of MCM-41 MSNs before and after the drug loading were reported. Both the isotherm of MCM-41 MSNs shows typical type IV isotherm according to IUPAC classification represents the mesoporosity. The isotherm recorded for MCM-41 MSNs also shows a hysteresis loop at high relative pressure, which has been ascribed to the presence of inter particle porosity[14, 15].

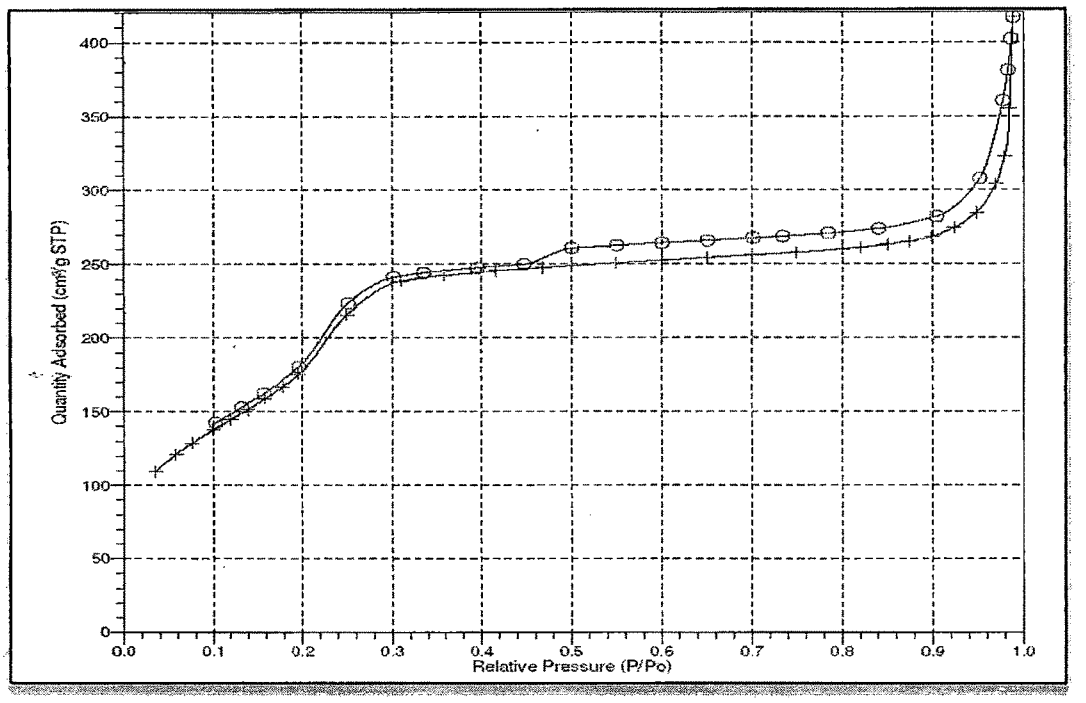

Figure 7.13-a: Nitrogen adsorption isotherm of MCM-41 MSNs before the drug loading

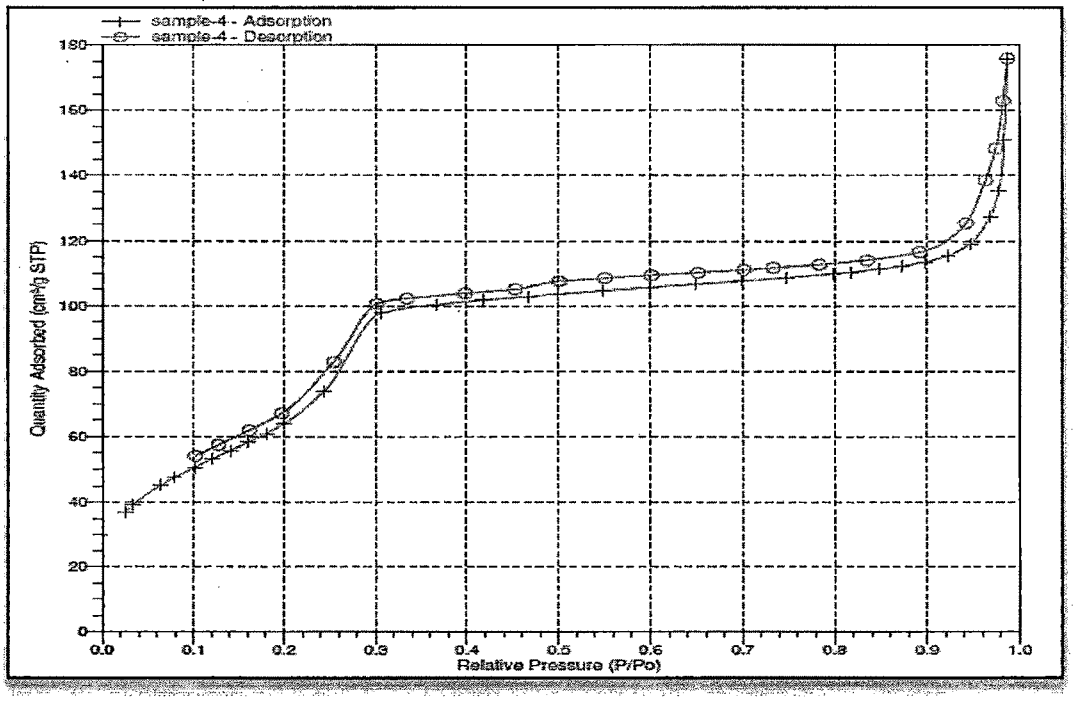

Figure 7.13-b: Nitrogen adsorption isotherm of MCM-41 MSNs after the drug loading

The calculated B.E.T. specific surface area for MCM-41 MSNs alone and MCM-41 MSNs after DTB loading were found to be 739.673 and 257.411 m^2/g, respectively. The adsorption isotherms of DTB loaded MSNs showed that the adsorbed nitrogen volume decreased after drug loading. Correspondingly, the average pore size distribution for drug loaded MCM-41 MSNs, calculated by the BJH–KJS method, was shifted from 3.69 nm to ca. 2.51 nm and the mesopore volume decreased from 0.470 to 0.197 cm^3/g for the primitive MCM-41 MSNs and drug loaded MCM-41 MSNs, respectively (Fig. 7.14). Numerical data are shown in Table 7.8 for MCM-41 MSNs and drug loaded MCM-41 MSNs.

Table 7.8: Pore diameter, volume and BET surface area of MCM-41 MSN

MSNs	Pore diameter (nm)	Pore volume (cm^3/g)	SBET (m^2/g)
MCM-41	3.696	0.470	739.671
DTB loaded MCM-41	2.511	0.197	257.411

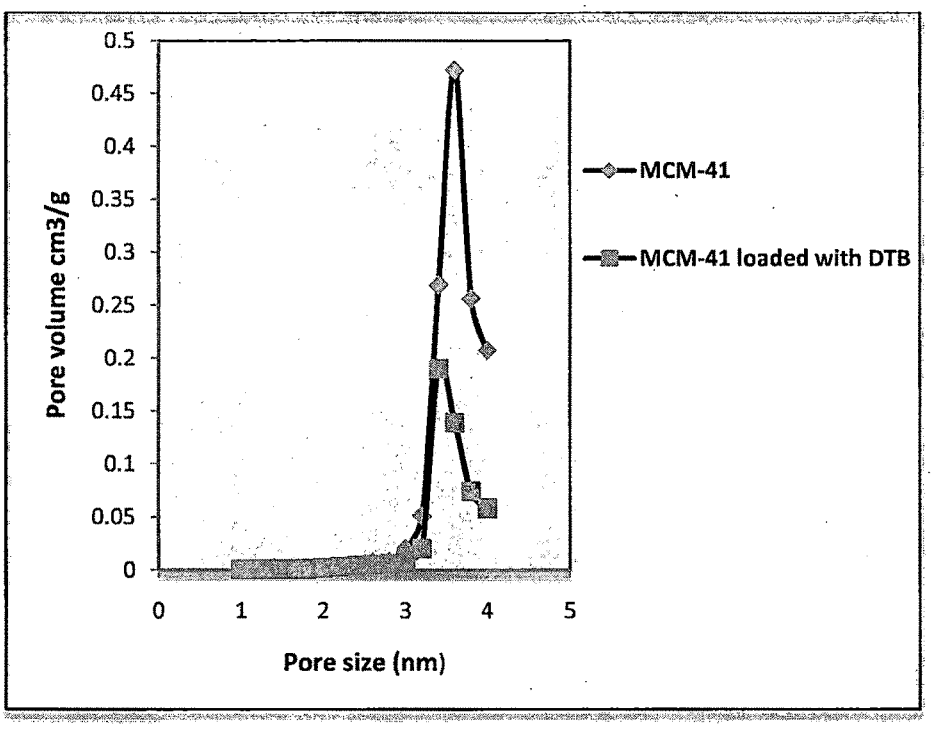

Figure 7.14: Pore size distribution and pore volume of MCM-41 MSN before and after drug loading

7.5.3.4 FTIR analysis

FTIR spectrum of MCM-41 MSNs (Fig. 7.16) showed the presence of a vibration band at 3740 cm^{-1} attributable to isolated terminal silanol groups and of another large band at 3611 cm^{-1} attributable to geminal and associated terminal silanol groups. The stretching vibrations of Si-O-Si and Si-OH can be seen at 1070 and 958 cm^{-1}. The FTIR spectral analysis of DTB powder (Fig. 7.15) showed the principal peaks at about 772 cm^{-1} (aryl C-Cl stretching), 1184 cm^{-1} (– C=S stretching), 1573 cm^{-1} (-CO-NH), 1621 cm^{-1} (-CO stretching of –CO-NH) 1452, 1505 cm^{-1} (aryl system), 809 cm^{-1} (aromatic ring system), and 2944 cm^{-1} (-OH stretching) confirming the purity of the drug. The spectra of drug loaded MSU-H MSNs (Fig. 7.17) shows a remarkable absence of the peaks which were observed in DTB pure sample, suggesting that majority of DTB was entrapped in MSNs.

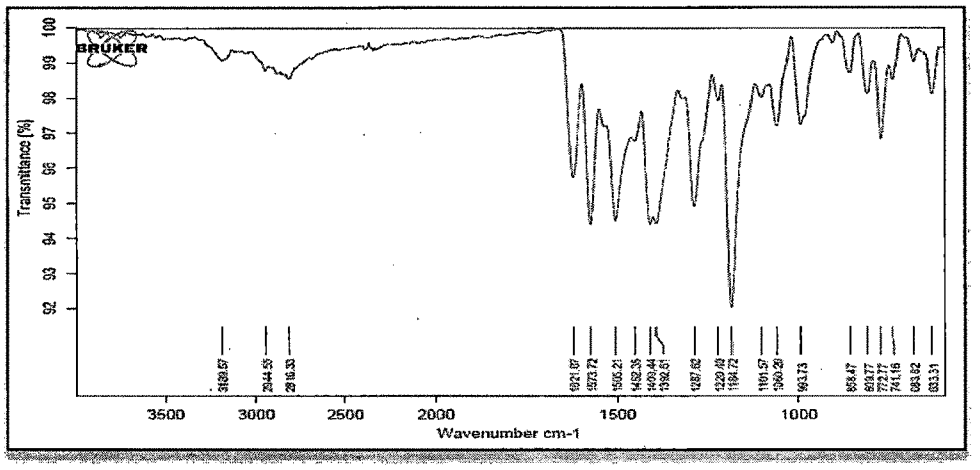

Figure 7.15: FTIR spectra of DTB

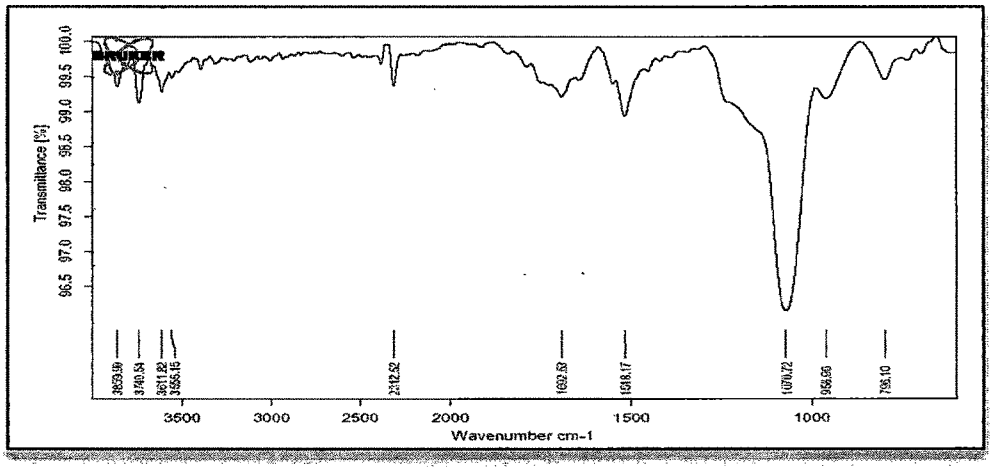

Figure 7.16: FTIR spectra of MCM-41 MSNs

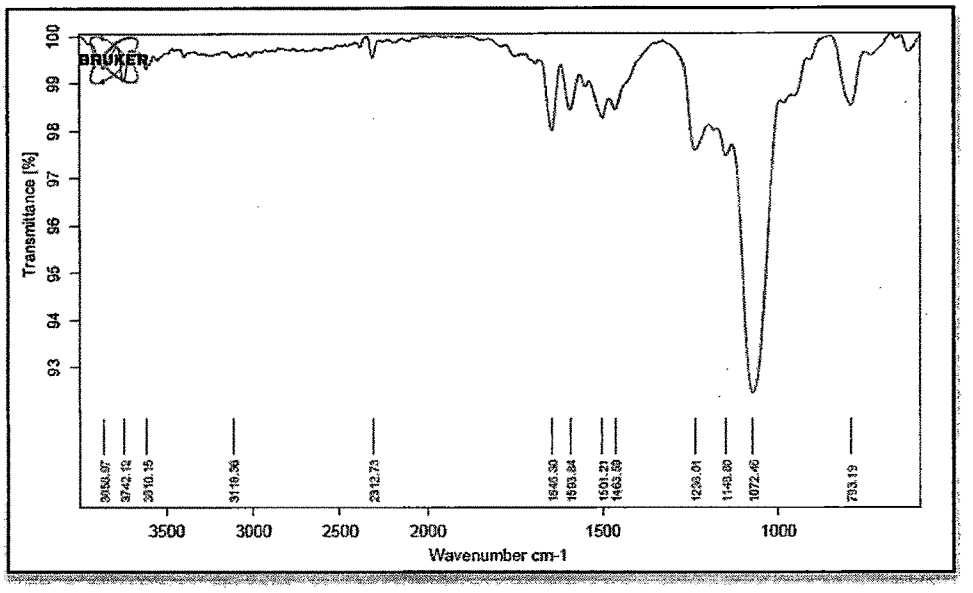

Figure 7.17: FTIR spectra of DTB loaded MCM-41 MSNs

7.5.3.5 Differential scanning calorimetry (DSC)

DSC thermograms were obtained to study the effectiveness of drug loading. The absence of endothermic peak in drug loaded MSNs is the indicative of the amorphous state as drug is confined within the pores.

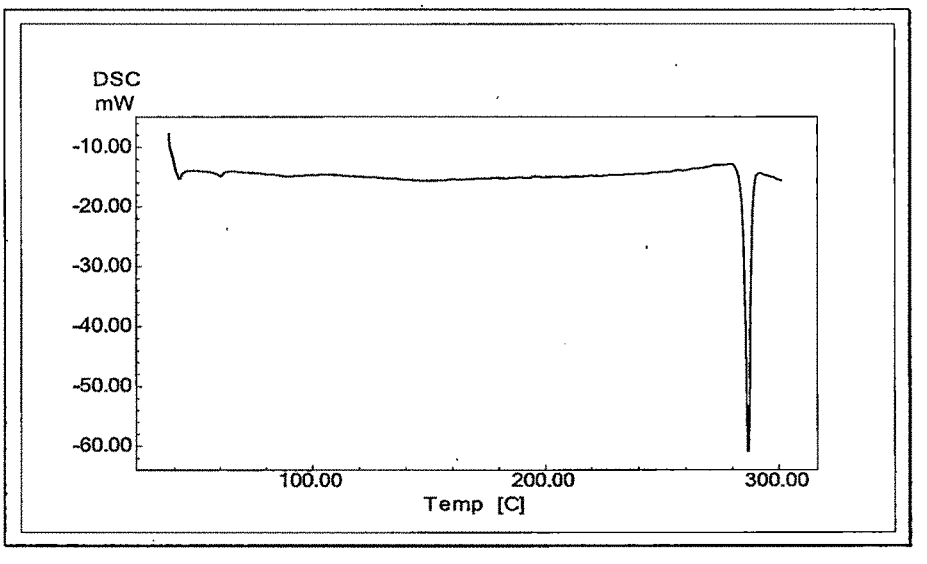

Figure 7.18: DSC thermogram of DTB

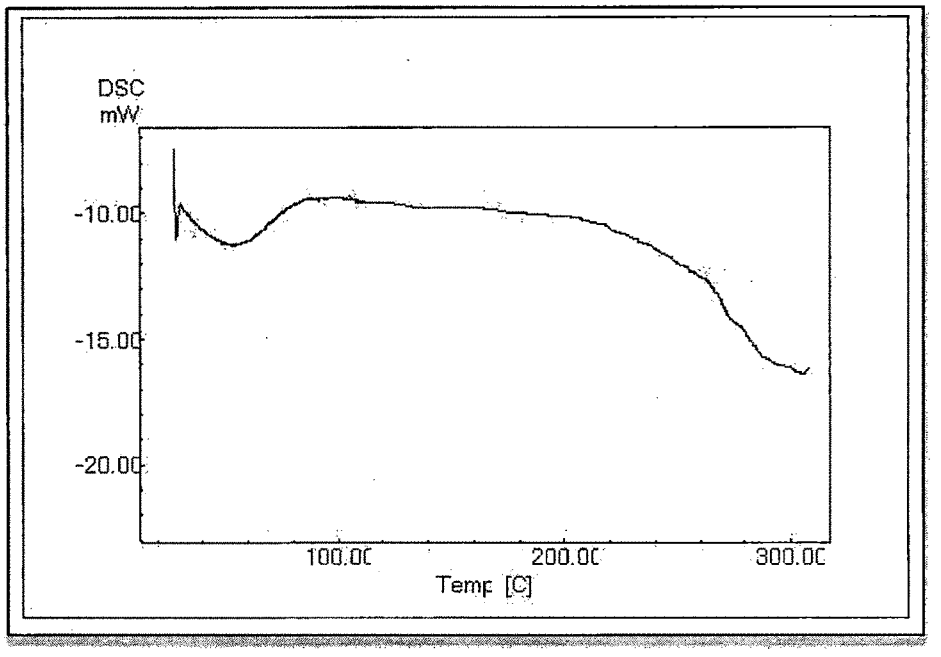

Figure 7.19: DSC thermogram of MCM-41 MSNs

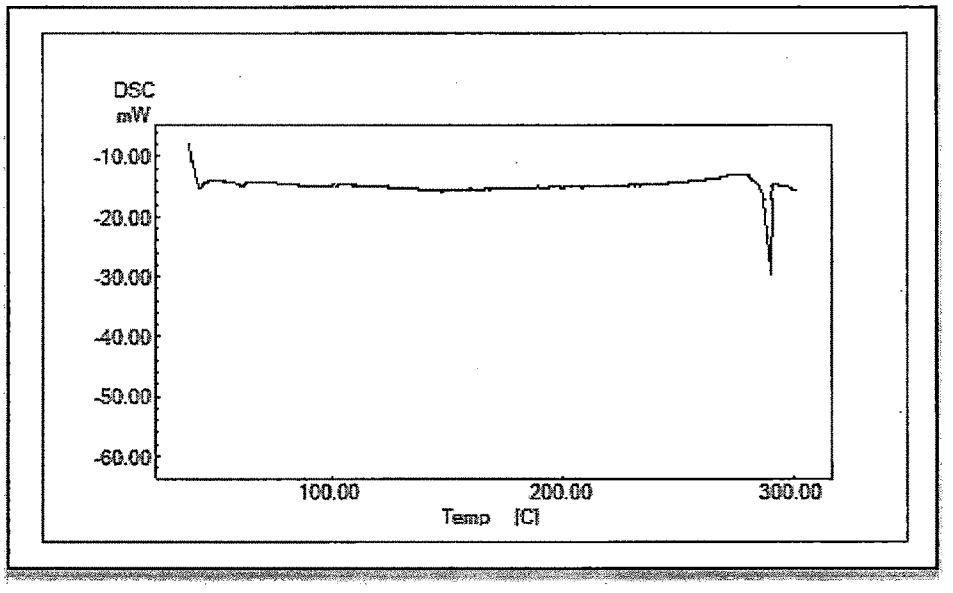

Figure 7.20: DSC thermogram of physical mixture of DTB and MCM-41 MSNs

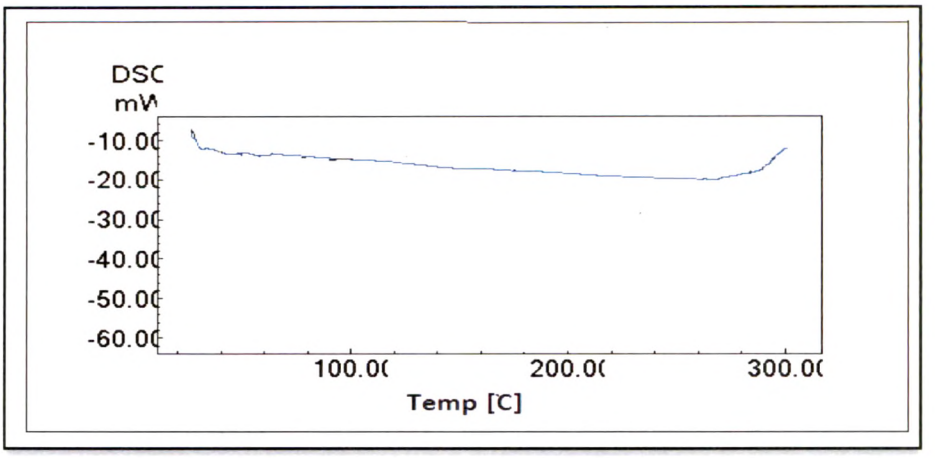

Figure 7.21: DSC thermogram of DTB loaded MCM-41 MSNs

Figure 7.18-7.21 shows DSC thermograms of MCM-41 MSNs, drug (DTB) loaded MCM-41 MSNs, physical mixture, and crystalline DTB. The DSC curve of DTB exhibited a single endothermic peak at 287 °C, which corresponded to its intrinsic melting points. Physical mixture of drug and MSNs show the less intense peak at 287 °C, indicated that drug molecules are not confined within the pores and drug was present in it crystalline state. However, no melting peak of DTB was identified in the DSC curves obtained from drug loaded MSNs. The absence of phase transitions owing to DTB in the DSC analysis is evidence that DTB is in a non-crystalline state.

7.6 *In-Vitro* dissolution study

Dissolution tests were performed at different pH conditions in order to investigate the drug release behavior in different regions of gastrointestinal tract. DTB dissolution from MCM-41-DTB was compared with those from DTB crystalline powder, physical mixture and marketed formulation (Fig. 7.23 (a–e)). In all test conditions DTB release from MCM-41 MSNs had a more rapid burst effect than the pure powder, physical mixture and marketed formulation. Schematic presentation of drug release from MCM-41 MSNs was shown in Fig. 7.22.

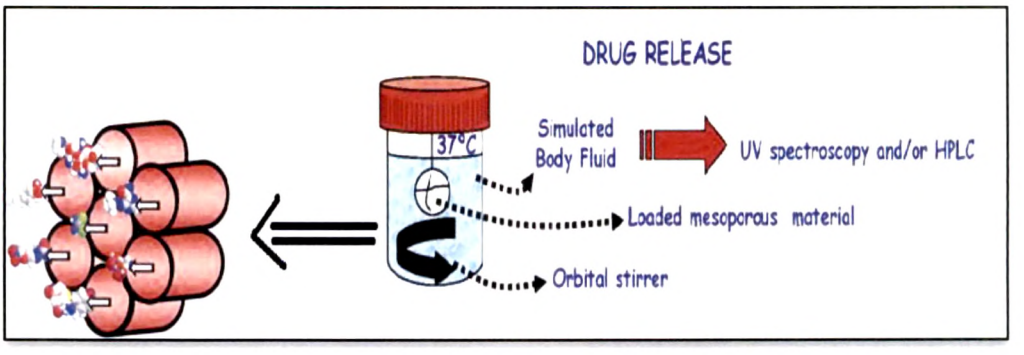

Figure 7.22: Schematic presentation of drug release from MCM-41 MSNs

The dissolution improvement may be largely attributed to the pore channels of the carriers i.e. MCM-41 MSNs, changing the crystalline state of DTB to an amorphous state, which is known to improve the drug solubility and dissolution rate[16-18]. In addition, the particle sizes of the amorphous drug incorporated in the pore channels (nano meter range) were significantly reduced compared with that of pure crystalline DTB (micron range). It is evident that a further decrease in the particle size to the nano meter range will further accelerate the drug release profile and, consequently, improve the dissolution rate[16-18].

Table 7.9 and 7.10 show the DTB release percentages at the tested pHs after 10 and 30 min respectively. The solubility of DTB is pH dependent; it can be observed that rapid release of the drug was more prominent in acidic media. In fact, in Acetate buffer pH 4 + Triton X-100 (1%) medium more than 70% of drug was released from MCM-41–DTB and a complete drug (100%) release was obtained after 10 and 30 min, whereas DTB dissolution from the crystalline powder was as low as 20% and 40% after 10 and 30 min respectively.

Table 7.9: Percentage of drug release after 10 minutes

Dissolution media	% drug release			
	Crystalline drug	Physical mixture	Marketed formulation	Developed formulation
Simulated gastric fluid pH 1.2	43.841	48.990	59.387	82.959
Phosphate buffer pH 4.5	1.804	5.336	10.628	20.520
Phosphate buffer pH 6.8	2.450	5.570	15.564	44.570
Simulated intest. fluid pH 7.4	0.031	4.262	10.421	11.712
Acetate buffer pH 4 + Triton X-100 (1%)	20.850	27.560	32.417	71.770

Table 7.10: Percentage of drug release after 30 minutes

Dissolution media	% drug release			
	Crystalline drug	Physical mixture	Marketed formulation	Developed formulation
Simulated gastric fluid pH 1.2	47.990	60.951	70.205	97.540
Phosphate buffer pH 4.5	12.613	41.250	47.148	59.152
Phosphate buffer pH 6.8	11.700	19.350	38.982	46.690
Simulated intest. fluid pH 7.4	1.261	9.065	15.849	21.172
Acetate buffer pH 4 + Triton X-100 (1%)	40.850	75.710	79.687	100.00

Finally, the DTB dissolution profile from MCM-41–DTB was compared to that of DTB from commercial formulation. The dissolution profiles indicate that after the 10 min, more than 70% drug was released from MCM-41–DTB whereas only 32% drug was released from the commercial tablet formulation of DTB. Similarly after 30 min drug release from marketed formulation was found to be 79% whereas complete release was obtained from the developed formulation.

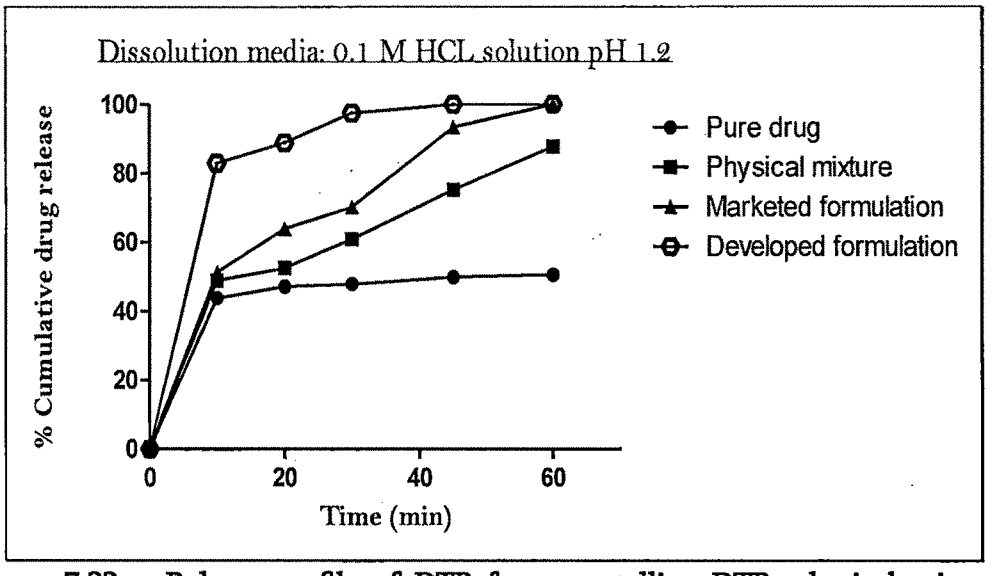

Figure 7.23-a: Release profile of DTB from crystalline DTB, physical mixture, marketed formulation, and developed formulation in pH 1.2

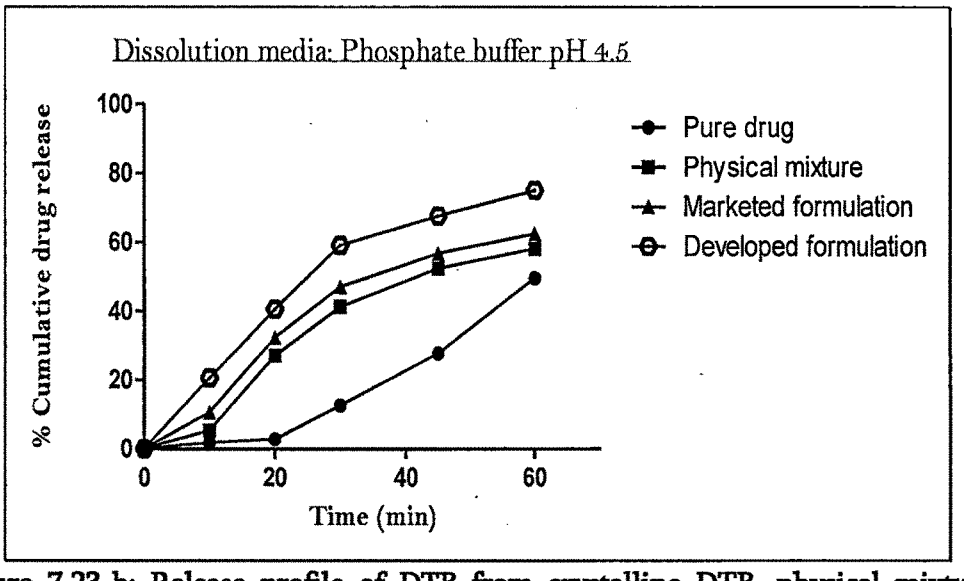

Figure 7.23-b: Release profile of DTB from crystalline DTB, physical mixture, marketed formulation, and developed formulation in pH 4.5

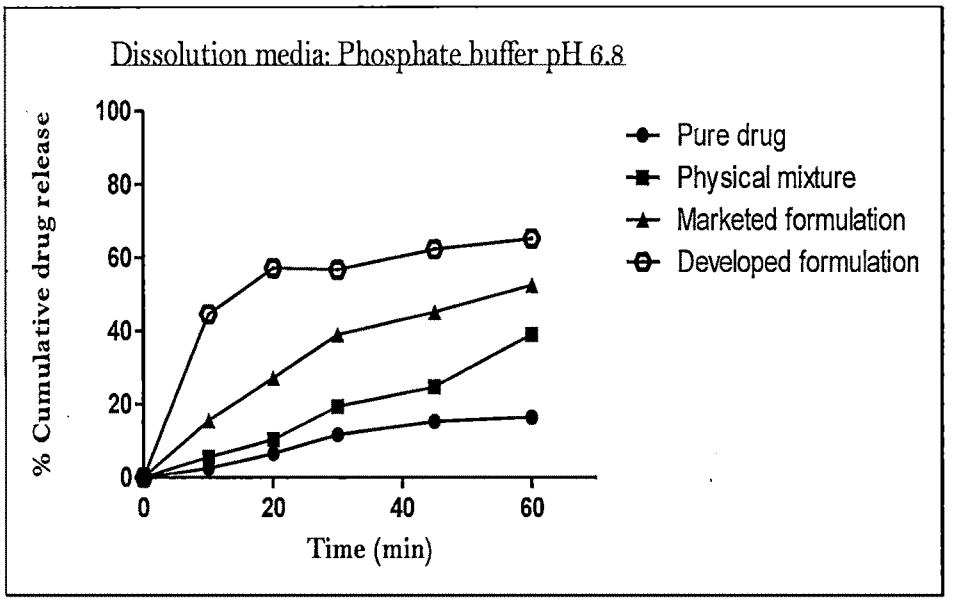

Figure 7.23-c: Release profile of DTB from crystalline DTB, physical mixture, marketed formulation, and developed formulation in pH 6.8

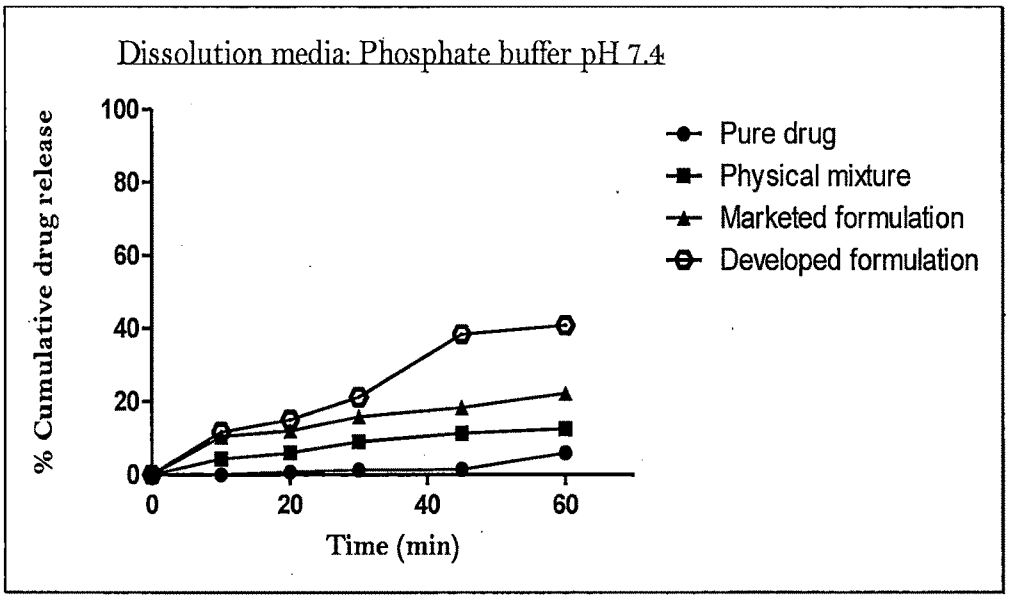

Figure 7.23-d: Release profile of DTB from crystalline DTB, physical mixture, marketed formulation, and developed formulation in pH 7.4

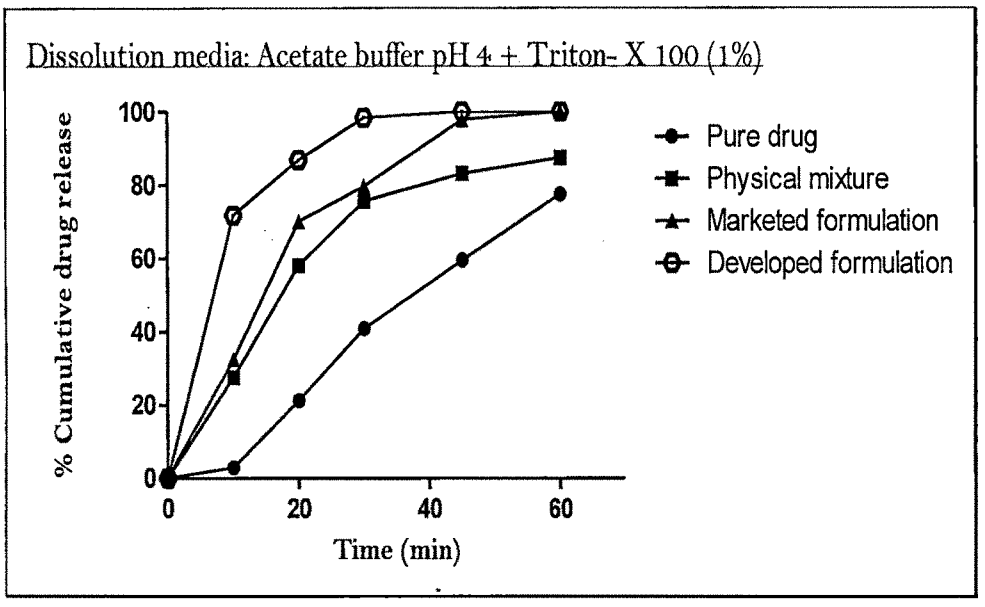

Figure 7.23-e: Release profile of DTB from crystalline DTB, physical mixture, marketed formulation, and developed formulation in reported media

References:

1 Wujun Xu, Qiang Gao, Yao Xua, Dong Wu, Yuhan Sun, Wanling Shen, Feng Deng. Controllable release of ibuprofen from size-adjustable and surface hydrophobic mesoporous silica spheres. Powd Tech. 2009; 191: 13-20.

2 Fish WP, Young J, Shah P, Gao Z. The use of experimental design principles in dissolution method development: development of a discriminating dissolution method for sprycel film-coated tablets. J Pharm Innov. 2009; 9: 9071-9075.

3 Ambrogia V, Perioli L, Marmottinib F, Giovagnolia S, Espositoa M, Rossia C. Improvement of dissolution rate of piroxicam byinclusion into MCM-41 mesoporous silicate. Eur J pharm Sci. 2007; 32: 216–222.

4 Haoualaa A, Zanolaria B, Rochatb B, Montemurrod M, Zamand K, Duchosale MA, Risc HB, Leyvrazd S, Widmera N, Decosterda LA. Therapeutic drug monitoring of the new targeted anticancer agents imatinib, nilotinib, dasatinib, sunitinib, sorafenib and lapatinib by LC tandem mass spectrometry. J Chromatogr B. 2009; 877: 1982–1996.

5 Schulz-Ekloff G, Rathousky J, Zukal A. Controlling of morphology and characterization of pore structure of ordered mesoporous silica. Micropor Mesopor Mater. 1999; 27: 273–285.

6 Griesser U.J, The importance of solvates. In Hilfiker R, ed. Polymorphism. Wiley-VCH Verlag GmbH & Co. KGaA, Weinheim, 2006; 211–233.

7 CRC handbook of solubility parameters and other cohesion parameters, A. F. M. Barton, ed., 2nd ed., CRC Press cop, Boca Raton (FL), 1991.

8 Bhattachar SN, Deschenes LA, Wesley JA. Solubility: it's not just for physical chemists. Drug Dis Today. 2006; 11: 1012–1018.

9 Bennema P, Van J, Van W, Los JH, Meekes H. Solubility of molecular crystals: Polymorphism in the light of solubility theory. Int J Pharm. 2008; 351: 1–2, 74–91.

10 Vandervoort J, Ludwig A. Preparation factors affecting the properties of polylactide nanoparticles: a factorial design study. Pharmazie. 2001; 56: 484- 488.

11 Box G, Hunter W, Hunter J. Statistics for experiments, John Wiley and Sons, New York, 1978; 291–334.

12 Cochran W.G, Cox G.M. Experimental Designs, second ed., John Wiley and Sons, New York, 1992; 335–375.

13 Miguel M, Maria V. New developments in ordered mesoporous materials for drug delivery J Mater Chem. 2010; 20: 5593–5604.

14 Brunauer S, Emmet P, Teller E. Adsorption of gases in multi molecular layers. J Am Chem Soc. 1938; 60: 309–319.

15 Choma J, Jaroniec M, Burakiewicz-Mortka W, Kloske M. Critical appraisal of classical methods for determination of mesopore size distributions of MCM-41 materials. Appl Surf Sci. 2002; 196: 216–223.

16 Salonen J, Laitinen L, Kaukonen AM, Tuura J, Björkqvist M, Heikkilä T, Vähä-Heikkilä K, Hirvonen J, Lehto V.P. Mesoporous silicon microparticles for oral drug delivery: loading and release of five model drugs. J Control Rel. 2005; 108: 362–374.

17 Heikkilä T, Salonen J, Tuura J, Kumar N, Salmi T, Murzin D.Y, Hamdy M.S, Mul G, Laitinen L, Kaukonen A.M, Hirvonen J, LehtoV. Evaluation of mesoporous TCPSi, MCM-41, SBA-15, and TUD-1 materials as API carriers for oral drug delivery. Drug Deliv. 2007; 14: 337–347.

18 Vasconcelos T, Sarmento B, Costa P. Solid dispersions as strategy to improve oral bioavailability of poor water soluble drugs. Drug Discov Today. 2007; 12: 1068–1075.